

Journal of Pakistan Institute of Chemical Engineers



journal homepage: www.piche.org.pk/journal

DOI: https://doi.org/10.54693/piche.05215



Tailored Polyether Sulfone/Cellulose Acetate Based Mixed Matrix Membranes for Enhanced Crude Glycerin Purification

S. Ahmad¹, Z. Asrar¹, B. Haider¹⁵, S. N. Hussain¹ Submitted: 17/05/2024, Accepted: 29/08/2024, Published: 30/08/2024

Abstract

Membrane based purification of crude glycerin is of unique importance due to its vast applications in pharmaceutical, polymer and food industries. Polyether Sulfone/Cellulose Acetate Based Mixed Matrix Membranes being reinforced with modified activated carbon has shown enough capability to purify crude glycerin. The membrane is synthesized by phase inversion method by using N- Methyl-2-pyrrolidone (NMP) as solvent and aminopropyl-triethoxycyclene as crosslinker. After adding modified activated carbon as a filler, the membrane is characterized using Fourier Transform Infrared (FTIR) spectroscopy and Thermal Gravimetric Analysis (TGA) to determine the chemistry and mechanical strength of the created membrane, respectively. All membranes' glycerin rejection is investigated using dead end filtration apparatus operating at two bar pressure. The impact of modified activated carbon is also examined by adjusting the filler concentration in a pure mixed matrix membrane solution. As a result, it is noted that the greatest glycerin rejection of 72.7% is achieved at 0.6% weight percentage of activated carbon. Nonetheless, at 0.8% weight of filler, a maximum water flux of 17.8 kg/hr.m2 was attained.

Keywords: Glycerin Rejection, N-Methyl-2-pyrrolidone (NMP), aminopropyl- triethoxycyclene, Phase Inversion.

1. Introduction:

An uncontrollable increase in population leads to unstoppable human activity. Fossil fuel depletion is one of the disastrous impacts of population expansion. Governments everywhere are attempting to reduce their reliance on fossil fuels. Reversing the trend away from crude oil and natural gas coal is now imperative, especially in the transportation and agricultural sectors(Khan et al., 2020) (Dilshad et al., 2020; Sabir et al., 2016). One such substitute is biodiesel, which is made from

biomass. One significant biodiesel byproduct is raw glycerin. One important factor in managing the quality of biodiesel is the quantity of free glycerin. Glycerin that has dissolved must be more than 0.02%; otherwise, problems with engine fuel injectors, decantation, and storage may arise (Shafiq et al., 2018). The consumption of glycerin in various products is shown in the Figure 1. This study's primary goals are to examine the benefits and possible applications of glycerin purification from biodiesel plants in the contemporary era.

Corresponding Author Email: bilal.icet@pu.edu.pk

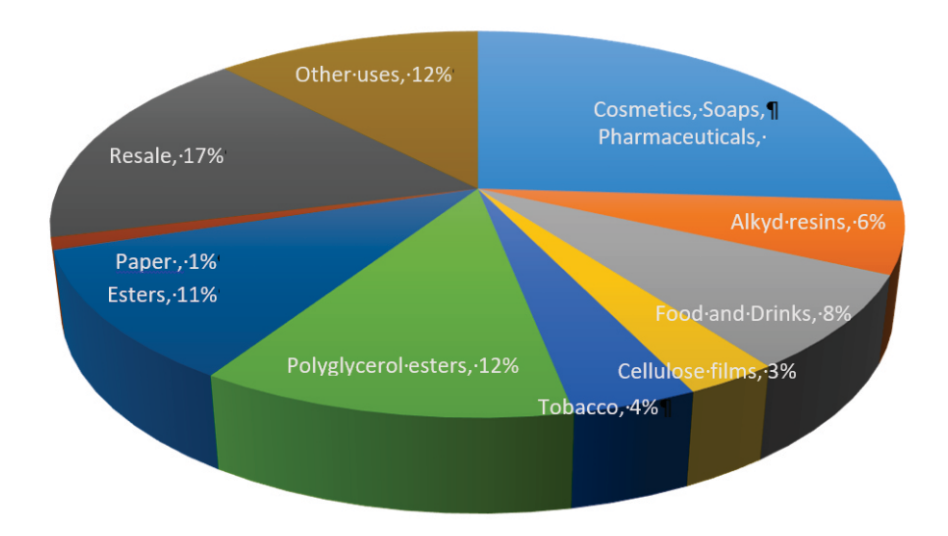


Figure 1: Consumption of glycerin in various products

Enhancing glycerin's usability is the primary motivation behind its purification. According to purity and possible end use, there are typically three technical level grades of glycerin accessible on the market (Ahmad et al., 2022; Ashraf et al., 1234; Sabir, Shafiq, et al., 2015). Table 1 lists various glycerin grades and their corresponding glycerin contents.

Table 1: General specification of glycerin in accordance to grade

Types of Glycerin	Glycerin amount (%)
Unrefined glycerin	70-90%
Technical leve	199.5 %(not certified mostly > 96.0%
USP grade	99.5% USP(tallow-based)
	99.5% USP(vegetable-based
FCC grade	99.7%USP/FCC-Kosher

These days, methods such as neutralization, crystallization, vacuum distillation, and ion exchange resin have become increasingly important for the separation and purification of crude glycerin. These efforts have accelerated as a result of research institutions discovering fresh concepts, methodologies, and projects in a variety of fields (Jamshaid, Dilshad, et al., 2020; Koriem et al., 2024). Activated carbon adsorption is often the last stage of glycerin purification. It was shown that adding more activated carbon significantly affected the refined crude glycerin's ability to remove color. Precise glycerol purification is achieved via membrane separation technique. Most isothermal membranes are driven by concentration gradient, hydrostatic pressure, and

electrical potential (H. Ali et al., 2022; Boussemghoune et al., 2020). Membranes are used in several

processes, such as reverse osmosis (RO), electrodialysis (ED), nanofiltration (NF), ultrafiltration (UF), and microfiltration (MF).

The glycerin rejection can be calculated by following expression.

$$R(\%) = (1 - \frac{C_p}{C_f}) \times 100 \rightarrow (1)^4$$

R is glycerin Rejection in terms of percentage, Cp is concentration of permeate and Cf is concertation of feed solution.

Purification of raw glycerol using a membrane contactor is a potentially helpful method.

Membrane separation technology has advanced with the use of membrane distillation. While typical membranes are driven by pressure, membrane distillation uses heat to drive the membrane process (Batool et al., 2021a; Liang et al., 2021). The majority of modern membrane distillation applications use a porous, non-wetting hydrophobic membrane to transfer water vapor for the purpose of extracting water. The major force behind the membrane distillation process would be a vapor pressure gradient created by the temperature gradient across the membrane. Given that both organic and ceramic membranes have shown the potential for the treatment of unrefined biodiesel products, it is notable that membrane technology has been utilized in the biodiesel manufacturing sector (Salehi et al., 2017; Zeeshan et al., 2021)

2. Material and methods:

2.1 Material

The polymeric materials utilized in the research are as follows:

2.1.1 Polyether sulfone (PES):

PES is a transparent, amorphous thermoplastic that is a member of the polysulfone family of high-temperature engineering thermoplastics. Solid, tough, and resilient, it holds its shape over a wide variety of temperatures. It has Tg = 225 °C and MW = 75,000 g/mol. PES from Ultra son® E 6020 was provided by BASF (Ludwigshafen, Germany) for use in this research project.

2.1.2 Cellulose Acetate:

Wood fibers and the small fibers (linters) that cling to cotton seeds are two natural sources of cellulose. It is made up of repeating glucose units with the chemical formula $C_6H_7O_2$ (OH) $_3$ and Mw = 102.09 g/mol. The molecular structure is displayed below. The source of the cellulose acetate utilized in this project is Acros Organics in Geel, Belgium.

2.1.3 N-Methyl-2-pyrrolidone (NMP):

Polar solvent N-Methyl-2-pyrrolidone (NMP) is widely used in pharmaceutical and industrial contexts. NMP has evolved into a typical solvent component of in situ developing implants for long-term medication delivery because of its safety profile at recognized concentrations. In a variety of

applications, it can function as a complexing agent and co-solvent.

2.2 Synthesis of Membrane:

Combine 10 g of PES and 80 g of NMP to get a homogeneous polymeric solution. In a similar way, another polymeric solution was made using 20g of cellulose acetate and 80g of NMP. Over the period of three to four days, the solutions were permitted to completely combine into a homogeneous mixture with sporadic stirring. A pure mixed membrane was produced by combining 1 g of cellulose acetate/NMP solution and 19 g of polyether sulfone/NMP solution after a homogeneous mixture had been created. The solution was agitated for 30 minutes and then sonicated for 30 minutes before the membrane was cast (Bahrodin et al., 2021; Batool et al., 2021b; She et al., 2015). Phase-inversion was used to generate the membranes, and once they were skinned off, they were completely submerged in distilled water for three days to remove any remaining solvent. Following creation, the membranes underwent a fifteen-minute immersion in methanol post-treatment (Sánchez-Moya et al., 2020).

2.3 Modification of Activated Carbon (AC):

2g of activated carbon should be combined with 150 ml of toluene and sonicated to change it. Following that, 150 microliters of cross linkers, also known as aminopropyl-triethoxycyclene, were added. For six hours, the mixture was continually stirred and the temperature was maintained between 60 and 65 °C. It is then centrifuged at 1000 rpm, washed with ethanol, and dried in an oven at 80–90 °C for 12 hours, according to Jamshaid, Rizwan Dilshad, et al. (2020).

2.4 Preparation of Membrane by Varying Modified Activated Carbon Compositions:

By combining 19 g of PES/NMP with 1 g of CA/NMP and adjusting the modified activated carbon content between 0.2 and 1% (w/w%) using the phase inversion method, a polymeric solution

combination was created (Silanikove et al., 2015).

To start, the necessary concentrations of a PES/CA solution were made. Following that, the mixture is agitated for approximately thirty minutes. The same adjusted AC concentration and a little amount of NMP, sufficient to dip the

activated carbon, are used to make a second solution. The solution AC/N 1MP is sonicated for 30 minutes prior to membrane casting (Dilshad et al., 2020). Table displays membrane with various amounts of AC.

Table 2. Membrane	with	varving	concentration	of	modified AC
Table 2. Membrane	** 1011	V 441 ,7 11115	COHCCHIUL GUION	OI	mountedire

Sr.	Membrane	NMP	PES	CA	Modified
					AC
		(W/W)%	(W/W)%	(W/W)%	%
1	P/C-0	80	19	1	0
2	P/C-0.2	80	19	1	0.2
3	P/C-0.4	80	19	1	0.4
4	P/C-0.6	80	19	1	0.6
5	P/C-0.8	80	19	1	0.8
6	P/C-1	80	19	1	1

2.1.1 Dead end filtration:

In this experiment, reverse osmosis is carried out using a home dead end filter (RO). A 26 cm² circular segment of membrane was gently inserted into the membrane support mesh. Two filter papers and one regular paper are positioned beneath the membrane to prevent the materials from mating. When the membrane is firmly in place, a ring and then a cylinder are inserted. One hundred milliliters of distilled water are added to the cylinder by actuating the feed valve. After that, nitrogen gas is pumped into the membrane at a pressure of 20 bar for 60 minutes. Ten bar of nitrogen was injected following the insertion of 100 ml of feed solution carrying 10, 20, 30, 40, and 50 g/L of glycerin through the feed valve (I. Ali et al., 2020; Zhang et al., 2020).

2.1.2 Fourier Transform Infrared Spectroscopy (FTIR):

This study uses Fourier Transform Infrared Spectroscopy (FTIR) to investigate the chemistry of pure polyether sulfone and cellulose acetate membranes in addition to mixed matrix polyether sulfone/cellulose acetate/activated carbon membranes. FTIR is based on the transmission and absorbance of infrared radiation, and it analyzes the components of the membrane material and measures the amount of chitosan

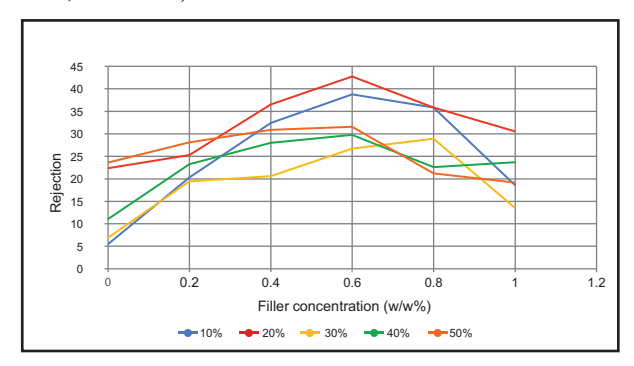
present. The FTIR spectrum of each membrane is distinct because different concentrations of chitosan in polyamide membranes have different bond energies and frequencies. The study uses 50 scans with an FTIR resolution of 4000 cm⁻¹ to 500 cm⁻¹.

3. Results and Discussions:

The effect of filler concentration on the rejection of glycerin, mean radius, water flux, solution flux and porosity are determined and analyzed.

3.1 Effect of Filler Concentration on the Rejection of Glycerin:

Various activated carbon concentrations (0%, 0.2%, 0.4%, 0.6%, 0.8%, and 1%), or filler, were examined, along with the tendency for rejecting glycerin solution concentrations (10%, 20%, 30%, 40%, and 50%).



 ${\bf Figure~2:}~{\bf Effect~of~filler~concentration~on~the~rejection~of~glycerin$

The filler cross-linking causes a significant decrease in rejection, which may also be caused by an increase in the concentration of glycerin solution, which acts as a barrier to rejection. Figure 2 illustrates a noticeable rise in rejection as the filler concentration gets raised up to 0.6 (w/w%). There achieves an optimum rejection of glycerin at particular filler concentration that decreases by further increasing the filler concentration.

3.2 Effect of Filler Concentration on the Flux of Solution:

Rise in filler concentrations causes the glycerin

solution flux to decrease because of the filler's interlinking and the increased glycerin concentration's impediment. The behavior is depicted in the Figure 3. The filler particles act as porogens and create more void spaces within the polymer matrix. Moreover, higher concentration of filler particles generally results in a larger total pore volume, providing more pathways for the solution molecules to pass through. Similarly, the permeability of membrane to solution improves due to least mass transfer resistance created in the presence of filler particles [10],[21].

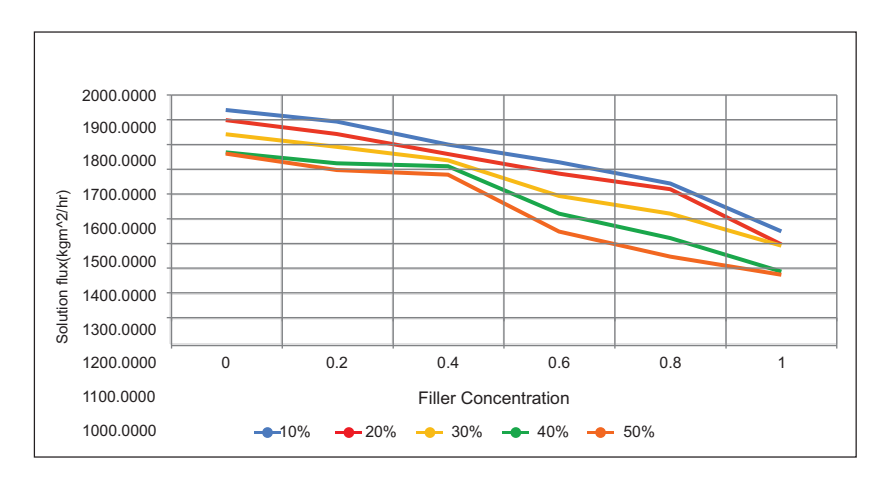


Figure 3: Effect of filler concentration on the solution flux

3.3 Effect of Filler Concentration on the Water Flux:

The decreasing trend of the glycerin concentration in Figure 4 is justified by the increasing trend of the water flux, which shows no obstruction and increases as the filler concentration rises. This is because as the glycerin concentration rises, the retentate contains more glycerin, which results in a decrease in the permeate flux [22], [23].

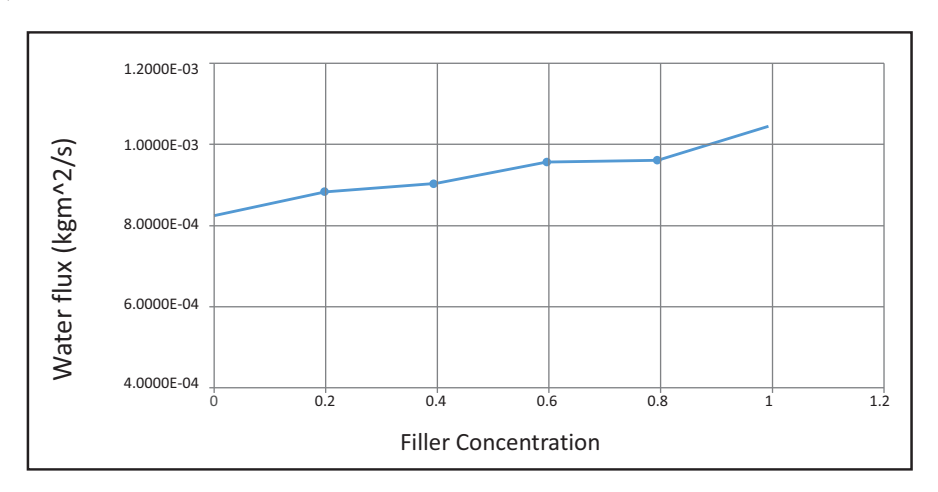


Figure 4: Effect of filler concentration on the water flux

3.4 Effect of Filler Concentration on the Mean Radius (rm)

The mean radius (rm) of the membrane's pores has been determined by the filler concentration. Figure 5 illustrates how the concentration of filler applied to the membrane causes a considerable rise in the mean radius of the membrane's pores. [1]

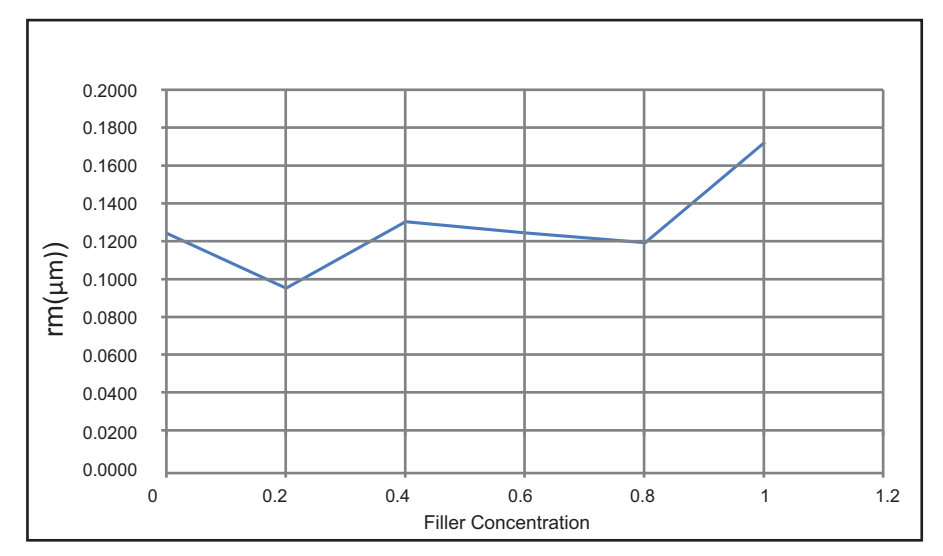


Figure 5: Effect of filler concentration on mean radius of membrane's pores

The particles of filler create void spaces around them and potentially increase pore radius. Similarly, low loading of filler leads to creation of void spaces. The shapes of filler particles have also direct effect on mean radius of pores. The spherical and irregular shaped particles create more pores and their irregular distribution. [24], [25], [26]

3.5 Effect of Filler Concentration on the Porosity of Membrane:

For a number of processes, the filler has been crucial

in determining the structure of the membrane. Figure 6 makes it evident that raising the filler concentration caused the membrane's pores to increase. The porosity of membranes increases by increasing the concentration of filler. The filler particles can act as porogens, creating void spaces around them during the membrane formation process. Moreover, the presence of filler particles disrupt the polymer matrix structure, leading to the formation of pores.[27],[28]

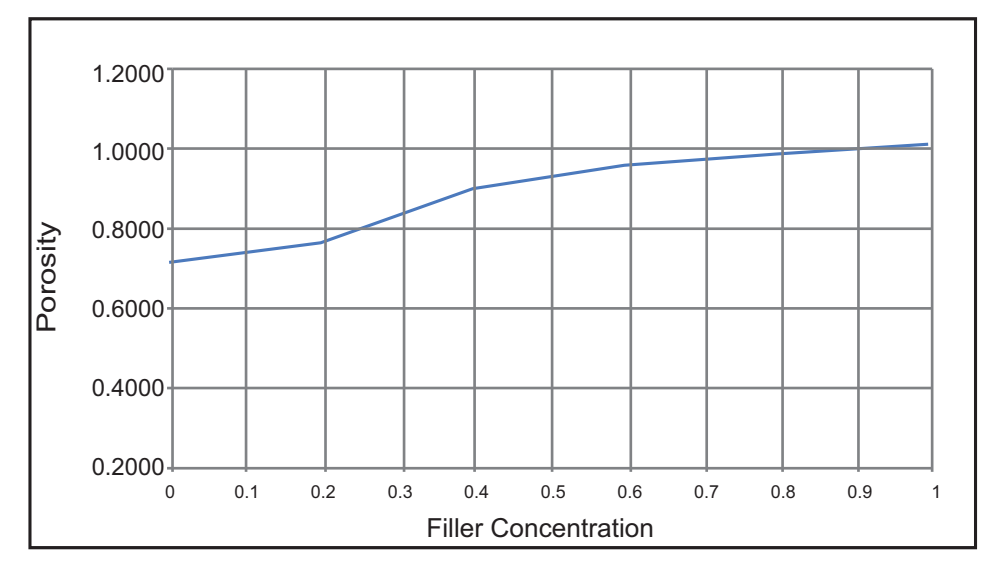


Figure 6: Effect of filler concentration on the porosity of membrane

3.6 Effect of the Porosity of Membrane on the Water Flux:

The graph illustrates how an increase in porosity causes a rise in water flux, as seen in Figure 7. Higher water flux in the event of increasing membrane porosity is caused by more paths and shorter path lengths. It does, however, lessen the membrane's capacity to reject undesirable substances. Hence, the presence of pores in

membrane accelerate the water flow from the membrane. The pores membrane has larger total surface area available for water molecules to pass through. Moreover, the higher porosity means least barriers for water molecules to encounter. Porosity is also directly linked to the permeability, which is a measure of how easily a fluid can pass through a material. [29], [30], [31].

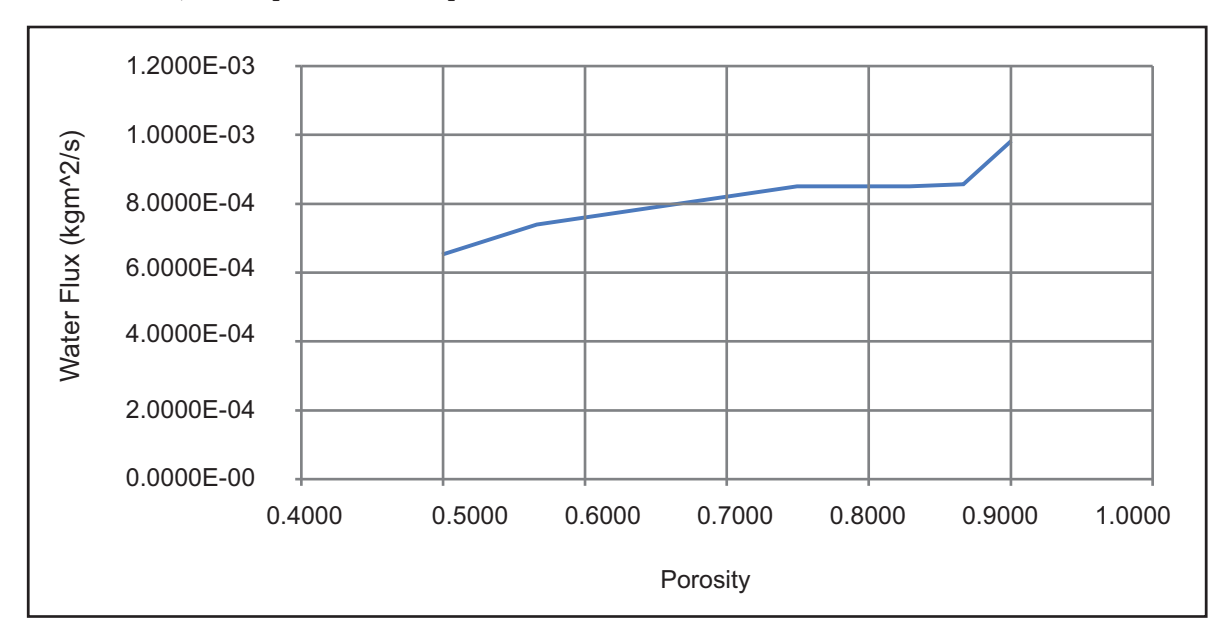


Figure 7: Effect of the porosity of membrane on the water flux

3.7 Fourier Transform Infrared Spectroscopy (FTIR):

FTIR spectroscopy was used to determine the membrane's surface functional groups. The stretching vibrations of OH groups is apparent by the large absorption band between $3300~{\rm cm}^{-1}$ and $3400~{\rm cm}^{-1}$, whereas the CH₂ groups are linked to the subsequent absorption peak at $2900~{\rm cm}^{-1}$

The water molecules that were absorbed as an outcome of a strong contact between the mixed matrix membrane and water are responsible for the absorption peak at 1640 cm⁻¹. As illustrated in Figure 8–13, the bands at 1169 cm⁻¹ and 895 cm⁻¹, respectively, are due to the C–O–C stretching (pyranose ring ether) and C–H rock vibration of cellulose (anomeric vibration of –glucosides).[12], [32].

The produced, pure PES membrane's FTIR spectra

displays absorption peaks at 1580 cm⁻¹ and 1480 cm⁻¹, respectively. These are linked to a phenyl groupether link and the C=C stretching vibration of benzene rings. Furthermore, the sulfone group in the PES base structure is shown by the absorption spectra at 1150 cm⁻¹ and 1100 cm⁻¹.

The spectra of the PES/CA/Activated carbon composite membranes were similar to those of virgin PES/CA membranes, especially between 1500 cm⁻¹ and 500 cm⁻¹. This pattern indicates that the composite membranes, as illustrated in Figure 8–13, can retain their PES/CA characteristics even in the presence of activated carbon. Significant fluctuations were seen in the peak region at 3398 cm⁻¹, 2898 cm⁻¹, and 1647 cm⁻¹, which correlate to the OH groups, CH₂ groups, and water absorbed, respectively.[33], [34]

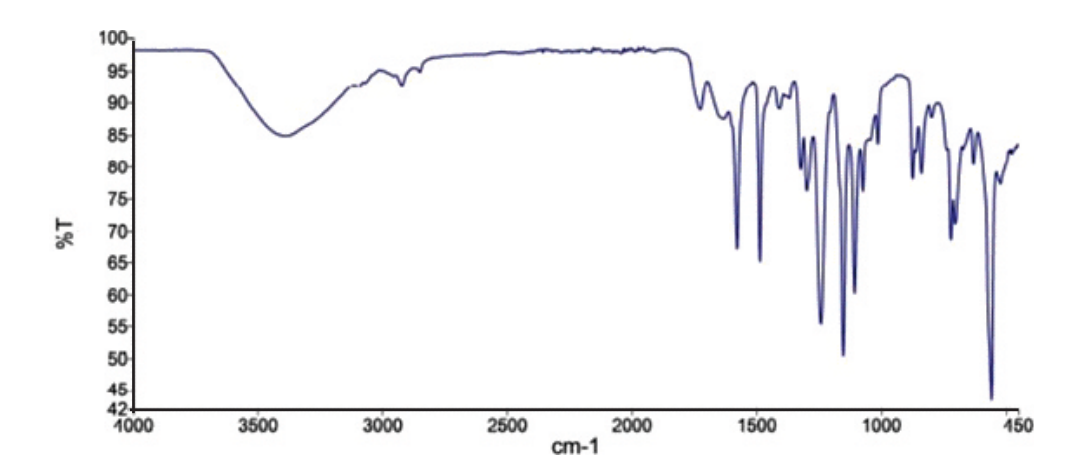


Figure 8: FTIR analysis of pure membrane

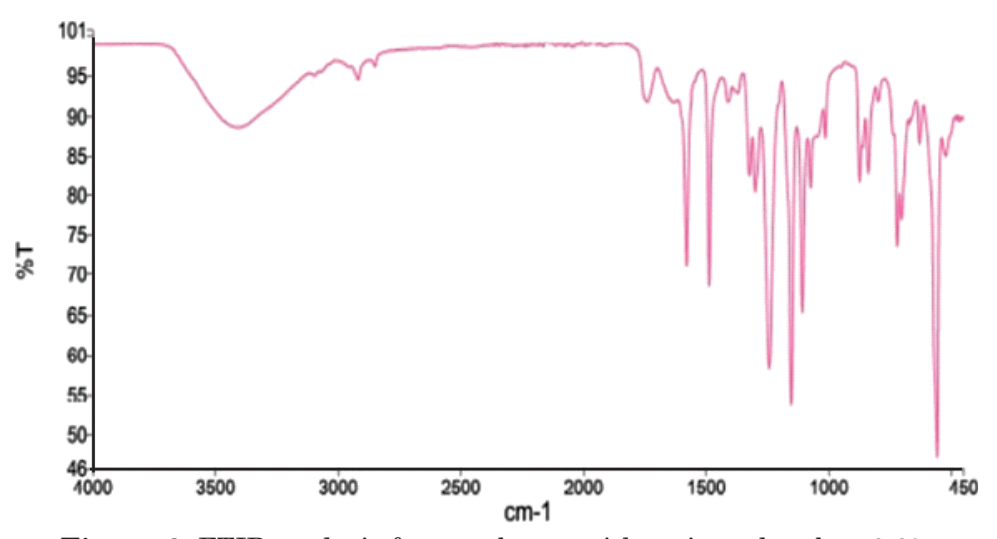


Figure 9: FTIR analysis for membrane with activated carbon 0.2%

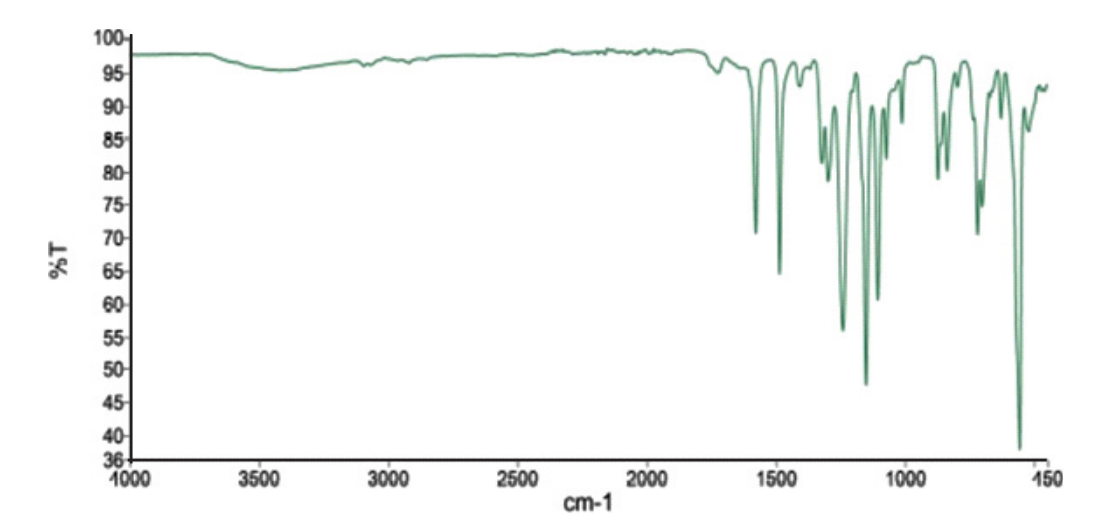


Figure 10: FTIR analysis for membrane with activated carbon 0.4%

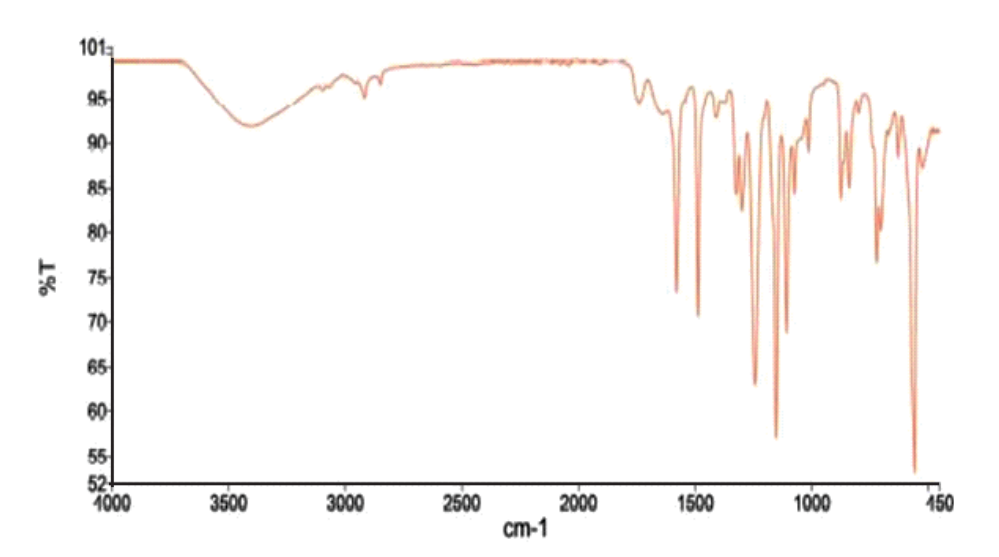


Figure 11: FTIR analysis for membrane with activated carbon 0.6%

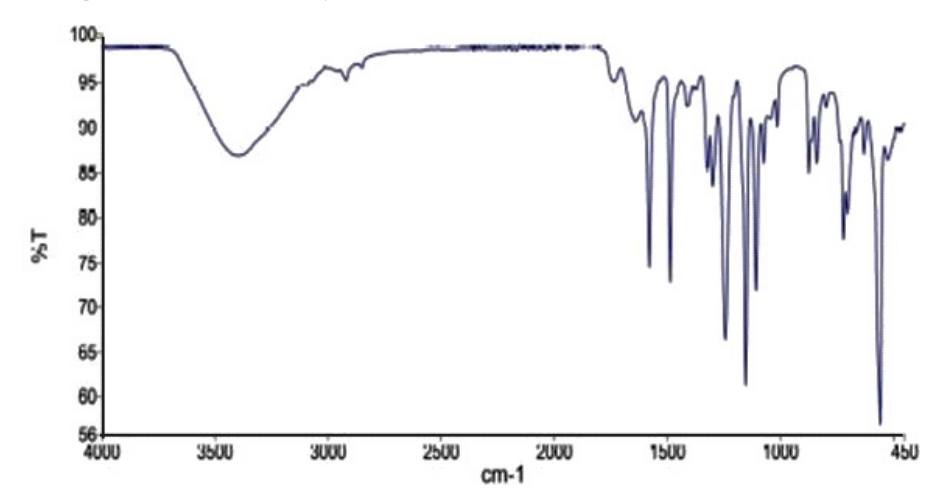


Figure 12: FTIR results for membrane with activated carbon 0.8%

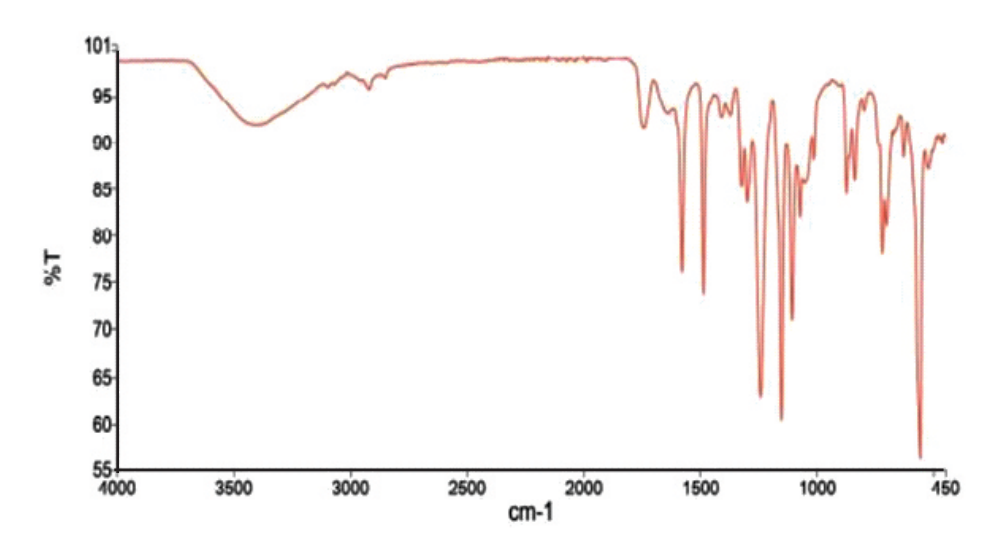


Figure 13: FTIR analysis of membrane with activated carbon 1 %

Conclusions:

It is explored how new Polyether Sulfone/Cellulose Acetate Based Mixed Matrix Membranes fortified with modified activated carbon can reject glycerin from solution. It has been found that the porosity of the membrane increased along with a surge in the filler concentration. In a similar vein, a little rise in the water flux is noted when the membrane's porosity increases. The connection between the filler concentration and the mean radius (rm) of the membrane's pores is not constant. Furthermore, a negative correlation has been observed between the concentration of modified activated carbon and water flux. It has been noted that a rise in filler concentration causes the water flux to gradually decline. On the other hand, the minimal filler concentration results in the largest water flux. The study of glycerin rejection takes into account variations in filler concentration. Research indicates that rejection rises as filler concentration rises. The concentration of zirconia at 0.6% is the highest at which glycerin rejection occurs. Nevertheless, as the filler content increases higher, glycerin rejection diminishes. Thus, crude glycerin can be purified using a PES/CA based mixed matrix membrane with an appropriate amount of modified activated carbon added as filler

References:

- M. K. Khan et al., "Selective Conversion of Carbon Dioxide into Liquid Hydrocarbons and Long-Chain α-Olefins over Fe-Amorphous AlO xBifunctional Catalysts," ACS Catal, vol. 10, no. 18, pp. 10325–10338, Sep. 2020, doi:10.1021/ACSCATAL.0C02611/SUPPL_FI LE/CS0C02611_SI_001.PDF.
- Z. 'Haider, B. 'Hussain, S. N. 'Asrar, "Tailored Polyether Sulfone/Cellulose Acetate Based Mixed Matrix Membranes for Enhanced Crude Glycerin Purification," University of the Punjab, Lahore, 2022.
- H. Zhang et al., "Preparation of Low-Lactose Milk Powder by Coupling Membrane Technology," 2020, doi: 10.1021/acsomega. 9b04252.
- 4. A. Sabir et al., "Novel polymer matrix

- composite membrane doped with fumed silica particles for reverse osmosis desalination," *Desalination*, vol. 368, pp. 159–170, Jul. 2015, doi: 10.1016/J.DESAL.2014.12.041.
- Q. She, R. Wang, A. G. Fane, and Y. Tang, "Membrane fouling in osmotically driven membrane processes: A review," 2015, doi: 10.1016/j.memsci.2015.10.040.
- 6. T. Sánchez-Moya, A. M. Hidalgo, G. Ros-Berruezo, and R. López-Nicolás, "Screening ultrafiltration membranes to separate lactose and protein from sheep whey: application of simplified model," *J Food Sci Technol*, vol. 57, no. 9, pp. 3193–3200, Sep. 2020, doi: 10.1007/S13197-020-04350-4/FIGURES/4.
- 7. H. Salehi, M. Rastgar, and A. Shakeri, "Antifouling and high water permeable forward osmosis membrane fabricated via layer by layer assembly of chitosan/graphene oxide," *Appl Surf Sci*, vol. 413, pp. 99–108, 2017, doi: 10.1016/j.apsusc.2017.03.271.
- M. Zeeshan et al., "Synergistic effect of silane cross-linker (APTEOS) on PVA/gelatin blend films for packaging applications," https://doi.org/10.1177/0954008321994659, vol. 33, no. 7, pp. 815-824, Feb. 2021, doi: 10.1177/0954008321994659.
- M. B. Bahrodin, N. S. Zaidi, N. Hussein, M. Sillanpää, D. D. Prasetyo, and A. Syafiuddin, "Recent Advances on Coagulation-Based Treatment of Wastewater: Transition from Chemical to Natural Coagulant," Curr Pollut Rep, vol. 7, no. 3, pp. 379–391, Sep. 2021, doi: 10.1007/S40726-021-00191-7/FIGURES/1.
- M. Batool, A. Shafeeq, B. Haider, and N. M. Ahmad, "TiO2 Nanoparticle Filler-Based Mixed-Matrix PES/CA Nanofiltration Membranes for Enhanced Desalination," *Membranes 2021, Vol. 11, Page 433*, vol. 11, no. 6, p. 433, Jun. 2021, doi: 10.3390/MEMBRANES 11060433.
- M. Batool, A. Shafeeq, B. Haider, and N. M. Ahmad, "TiO2 Nanoparticle Filler-Based Mixed-Matrix PES/CA Nanofiltration Membranes for Enhanced Desalination,"

- Membranes 2021, Vol. 11, Page 433, vol. 11, no. 6, p. 433, Jun. 2021, doi: 10.3390/MEMBRANES11060433.
- 12. S. Ahmad, B. Haider, and S. N. Hussain, "Adsorption of Crystal Violet Dye onto Anionic Polyacrylamide-Modified Graphite: Equilibrium, Kinetics, and Mechanism," ASEAN Journal of Chemical Engineering, vol. 24, no. 2, pp. 174–185, Aug. 2024, doi: 10.22146/ajche.12218.
- 13. N. Silanikove, G. Leitner, and U. Merin, "The Interrelationships between Lactose Intolerance and the Modern Dairy Industry: Global Perspectives in Evolutional and Historical Backgrounds," Nutrients, vol. 7, pp. 7312-7331, 2015, doi: 10.3390/nu7095340.
- 14. F. Jamshaid *et al.*, "Synthesis, characterization and desalination study of polyvinyl chloride-co-vinyl acetate/cellulose acetate membranes integrated with surface modified zeolites," 2020, doi: 10.1016/j.micromeso.2020.110579.
- 15. "Wastewater Treatment Technologies For The Textile Industry-FINAL PDF | PDF | Sewage Treatment | Membrane." Accessed: May 19, 2 0 2 4 . [Online]. Available: https://www.scribd.com/document/409198127/Wastewater-Treatment-Technologies-for-the-Textile-Industry-FINAL-pdf
- 16. Q. Wang, J. Cui, A. Xie, J. Lang, C. Li, and Y. Yan, "PVDF composite membrane with robust UV-induced self-cleaning performance for durable oil/water emulsions separation," J Taiwan Inst Chem Eng, vol. 110, pp. 130–139, May 2020, doi: 10.1016/J.JTICE.2020.02.024.
- 17. I. Ali et al., "Novel Maleic Acid, Crosslinked, Nanofibrous Chitosan/Poly (Vinylpyrrolidone) Membranes for Reverse Osmosis Desalination," International Journal of Molecular Sciences 2020, Vol. 21, Page 7338, vol. 21, no. 19, p. 7338, Oct. 2020, doi: 10.3390/IJMS21197338.
- M. Boussemghoune, M. Chikhi, F. Balaska, Y. Ozay, N. Dizge, and B. Kebabi, "Preparation of a zirconia-based ceramic membrane and its

- application for drinking water treatment," *Symmetry (Basel)*, vol. 12, no. 6, Jun. 2020, doi: 10.3390/SYM12060933.
- 19. M. Shafiq et al., "Cellulaose acetate based thin film nanocomposite reverse osmosis membrane incorporated with TiO2 nanoparticles for improved performance," Carbohydr Polym, vol. 186, pp. 367-376, Apr. 2018, doi: 10.1016/J.CARBPOL.2018.01.070.
- 20. A. Sabir et al., "Conjugation of silica nanoparticles with cellulose acetate/polyethylene glycol 300 membrane for reverse osmosis using MgSO 4 solution," Carbohydr Polym, vol. 136, pp. 551–559, 2016, doi: 10.1016/j.carbpol.2015.09.042.
- 21. S. K. Hubadillah et al., "Fabrication of low cost, green silica based ceramic hollow fibre membrane prepared from waste rice husk for water filtration application," Ceram Int, vol. 44, no. 9, pp. 10498–10509, Jun. 2018, doi: 10.1016/J.CERAMINT.2018.03.067.
- 22. M. A. Ashraf, A. Islam, · Muhammad, and A. Butt, "Novel Silica Functionalized Monosodium Glutamate/PVA Cross-Linked Membranes for Alkali Recovery by Diffusion Dialysis," *J Polym Environ*, vol. 30, pp. 516–527, 1234, doi: 10.1007/s10924-021-02205-3.
- 23. H. Ali et al., "Preparation and characterization of novel Polyamide-6/Chitosan blend dense membranes for desalination of brackish water," Polymer Bulletin, vol. 79, no. 6, pp. 4153–4169, Jun. 2022, doi: 10.1007/S00289-021-03691-0/TABLES/4.
- 24. A. Sabir *et al.*, "Fabrication of tethered carbon nanotubes in cellulose acetate/polyethylene glycol-400 composite membranes for reverse osmosis," *Carbohydr Polym*, vol. 132, pp. 589–597, Nov. 2015, doi: 10.1016/J.CARBPOL. 2015.06.035.
- 25. B. Ahmad *et al.*, "Synthesis of novel fly ash based geo-polymeric membranes for the treatment of textile waste water," *International Journal of Environmental Science and Technology*, vol. 19, no. 3, pp.

- 6117–6126, 2022, doi: 10.1007/s13762-021-03527-4.
- 26. S. Saberi, A. A. Shamsabadi, M. Shahrooz, M. Sadeghi, and M. Soroush, "Improving the Transport and Antifouling Properties of Poly(vinyl chloride) Hollow-Fiber Ultrafiltration Membranes by Incorporating Silica Nanoparticles," 2018, doi: 10.1021/acsomega.8b02211.
- 27. F. Jamshaid et al., "Synthesis, characterization and desalination study of polyvinyl chloride-co-vinyl acetate/cellulose acetate membranes integrated with surface modified zeolites," Microporous and Mesoporous Materials, vol. 309, p. 110579, Dec. 2020, doi: 10.1016/J.MICROMESO.2020. 110579.
- 28. M. R. Dilshad *et al.*, "Fabrication and performance characterization of novel zinc oxide filled cross-linked PVA/PEG 600 blended membranes for CO2/N2 separation," *Journal of Industrial and Engineering Chemistry*, vol. 55, pp. 65–73, Nov. 2017, doi: 10.1016/J.JIEC. 2017.06.029.
- M. R. Dilshad et al., "Effect of alumina on the performance and characterization of cross-linked PVA/PEG 600 blended membranes for CO2/N2 separation," Sep Purif Technol, vol. 210, pp. 627–635, Feb. 2019, doi: 10.1016/J.SEPPUR.2018.08.026.
- 30. H. Liang, C. Zou, and W. Tang, "Development of novel polyether sulfone mixed matrix membranes to enhance antifouling and sustainability: Treatment of oil sands produced water (OSPW)," *J Taiwan Inst Chem Eng*, vol. 118, pp. 215–222, 2021, doi: 10.1016/j.jtice.2020.12.022.
- 31. O. A. Koriem, M. S. Showman, A. H. El-Shazly, and M. Elkady, "Synthesis of highperformance biocompatible polymeric membranes incorporated with zirconium-based MOF for an enhanced brackish water RO desalination," *Cellulose*, vol. 31, no. 4, pp. 2309–2325, Mar. 2024, doi: 10.1007/S10570-023-05723-6/TABLES/3.

- 32. A. Raza *et al.*, "Synthesis and investigation of desalinating, antibacterial, and mechanical properties of tetraethylorthosilicate crosslinked chitosan/ polyethylene glycol (PEG-300) membranes for reverse osmosis," 2019, doi: 10.1002/app.48870.
- 33. S. Miao, J. Guo, Z. Deng, J. Yu, and Y. Dai, "Adsorption and reduction of Cr(VI) in water by iron-based metal-organic frameworks (Fe-MOFs) composite electrospun nanofibrous membranes," *J Clean Prod*, vol. 370, p. 133566, Oct. 2022, doi: 10.1016/J.JCLEPRO .2022.133566.
- 34. A. Kayani et al., "Effect of Varying Amount of Polyethylene Glycol (PEG-600) and 3-Aminopropyltriethoxysilane on the Properties of Chitosan based Reverse Osmosis Membranes," International Journal of Molecular Sciences 2021, Vol. 22, Page 2290, vol. 22, no. 5, p. 2290, Feb. 2021, doi: 10.3390/IJMS22052290.